CERN-PPE/96-10
29 January 1996

Search for supersymmetric particles in e^+e^- collisions at centre-of-mass energies of 130 and 136 GeV

The ALEPH Collaboration*)

Abstract

Searches for supersymmetric particles produced in e^+e^- collisions at centre-of-mass energies of 130 and 136 GeV have been performed in a data sample of 5.7 pb^{-1} collected in the autumn of 1995 by the ALEPH detector at LEP. No candidate events were found, allowing limits to be set on the masses and production cross-sections of scalar leptons, scalar tops, charginos and neutralinos. The domains previously excluded at LEP1 are substantially extended. For instance, masses of gaugino-like charginos smaller than 67.8 GeV/c^2 are excluded at the 95% C.L. for scalar neutrino masses larger than 200 GeV/c^2.

(Submitted to Physics Letters B)

*) See next pages for the list of authors

The ALEPH Collaboration

D. Buskulic, I. De Bonis, D. Decamp, P. Ghez, C. Goy, J.-P. Lees, A. Lucotte, M.-N. Minard, P. Odier, B. Pietrzyk

Laboratoire de Physique des Particules (LAPP), IN^{2}P^3-CNRS, 74019 Annecy-le-Vieux Cedex, France

M. Chmeissani, J.M. Crespo, M. Delfino,[12] I. Efthymiopoulos, E. Fernandez, M. Fernandez-Bosman, Ll. Garrido,[15] A. Juste, M. Martinez, S. Orteu, A. Pacheco, C. Padilla, A. Pascual, J.A. Perlas, I. Riu, F. Sanchez, F. Teubert

Institut de Fisica d'Altes Energies, Universitat Autonoma de Barcelona, 08193 Bellaterra (Barcelona), Spain[7]

A. Colaleo, D. Creanza, M. de Palma, G. Gelao, M. Girone, G. Iaselli, G. Maggi,[3] M. Maggi, N. Marinelli, S. Nuzzo, A. Ranieri, G. Raso, F. Ruggieri, G. Selvaggi, L. Silvestris, P. Tempesta, G. Zito

Dipartimento di Fisica, INFN Sezione di Bari, 70126 Bari, Italy

X. Huang, J. Lin, Q. Ouyang, T. Wang, Y. Xie, R. Xu, S. Xue, J. Zhang, L. Zhang, W. Zhao

Institute of High-Energy Physics, Academia Sinica, Beijing, The People's Republic of China[8]

R. Alemany, A.O. Bazarko, M. Cattaneo, P. Comas, P. Coyle, H. Drevermann, R.W. Forty, M. Frank, R. Hagelberg, J. Harvey, P. Janot, B. Jost, E. Kneringer, J. Knobloch, I. Lehraus, E.B. Martin, P. Mato, A. Minten, R. Miquel, Ll.M. Mir,[2] L. Moneta, T. Oest,[1] F. Palla, J.-F. Pusztaszeri, F. Ranjard, P. Rensing, L. Rolandi, D. Schlatter, M. Schmelling,[24] O. Schneider, W. Tejessy, I.R. Tomalin, A. Venturi, H. Wachsmuth, A. Wagner

European Laboratory for Particle Physics (CERN), 1211 Geneva 23, Switzerland

Z. Ajaltouni, A. Barrès, C. Boyer, A. Falvard, P. Gay, C . Guicheney, P. Henrard, J. Jousset, B. Michel, S. Monteil, J-C. Montret, D. Pallin, P. Perret, F. Podlyski, J. Proriol, J.-M. Rossignol

Laboratoire de Physique Corpusculaire, Université Blaise Pascal, IN^{2}P^3-CNRS, Clermont-Ferrand, 63177 Aubière, France

T. Fearnley, J.B. Hansen, J.D. Hansen, J.R. Hansen, P.H. Hansen, B.S. Nilsson, A. Wäänänen

Niels Bohr Institute, 2100 Copenhagen, Denmark[9]

A. Kyriakis, C. Markou, E. Simopoulou, I. Siotis, A. Vayaki, K. Zachariadou

Nuclear Research Center Demokritos (NRCD), Athens, Greece

A. Blondel, J.C. Brient, A. Rougé, M. Rumpf, A. Valassi,[6] H. Videau[21]

Laboratoire de Physique Nucléaire et des Hautes Energies, Ecole Polytechnique, IN^{2}P^3-CNRS, 91128 Palaiseau Cedex, France

D.J. Candlin, M.I. Parsons

Department of Physics, University of Edinburgh, Edinburgh EH9 3JZ, United Kingdom[10]

E. Focardi,[21] G. Parrini

Dipartimento di Fisica, Università di Firenze, INFN Sezione di Firenze, 50125 Firenze, Italy

M. Corden, C. Georgiopoulos, D.E. Jaffe

Supercomputer Computations Research Institute, Florida State University, Tallahassee, FL 32306-4052, USA [13,14]

A. Antonelli, G. Bencivenni, G. Bologna,[4] F. Bossi, P. Campana, G. Capon, D. Casper, V. Chiarella, G. Felici, P. Laurelli, G. Mannocchi,[5] F. Murtas, G.P. Murtas, L. Passalacqua, M. Pepe-Altarelli

Laboratori Nazionali dell'INFN (LNF-INFN), 00044 Frascati, Italy

L. Curtis, S.J. Dorris, A.W. Halley, I.G. Knowles, J.G. Lynch, V. O'Shea, C. Raine, P. Reeves, J.M. Scarr, K. Smith, A.S. Thompson, F. Thomson, S. Thorn, R.M. Turnbull

Department of Physics and Astronomy, University of Glasgow, Glasgow G12 8QQ,United Kingdom[10]

U. Becker, C. Geweniger, G. Graefe, P. Hanke, G. Hansper, V. Hepp, E.E. Kluge, A. Putzer, B. Rensch, M. Schmidt, J. Sommer, H. Stenzel, K. Tittel, S. Werner, M. Wunsch

Institut für Hochenergiephysik, Universität Heidelberg, 69120 Heidelberg, Fed. Rep. of Germany[16]

D. Abbaneo, R. Beuselinck, D.M. Binnie, W. Cameron, P.J. Dornan, A. Moutoussi, J. Nash, J.K. Sedgbeer, A.M. Stacey, M.D. Williams

Department of Physics, Imperial College, London SW7 2BZ, United Kingdom[10]

G. Dissertori, P. Girtler, D. Kuhn, G. Rudolph

Institut für Experimentalphysik, Universität Innsbruck, 6020 Innsbruck, Austria[18]

A.P. Betteridge, C.K. Bowdery, P. Colrain, G. Crawford, A.J. Finch, F. Foster, G. Hughes, T. Sloan, M.I. Williams

Department of Physics, University of Lancaster, Lancaster LA1 4YB, United Kingdom[10]

A. Galla, A.M. Greene, C. Hoffmann, K. Kleinknecht, G. Quast, B. Renk, E. Rohne, H.-G. Sander, P. van Gemmeren C. Zeitnitz

Institut für Physik, Universität Mainz, 55099 Mainz, Fed. Rep. of Germany[16]

J.J. Aubert,[21] A.M. Bencheikh, C. Benchouk, A. Bonissent,[21] G. Bujosa, D. Calvet, J. Carr, C. Diaconu, N. Konstantinidis, P. Payre, D. Rousseau, M. Talby, A. Sadouki, M. Thulasidas, A. Tilquin, K. Trabelsi

Centre de Physique des Particules, Faculté des Sciences de Luminy, IN^{2}P^3-CNRS, 13288 Marseille, France

I. Abt, R. Assmann, C. Bauer, W. Blum, H. Dietl, F. Dydak,[21] G. Ganis, C. Gotzhein, K. Jakobs, H. Kroha, G. Lütjens, G. Lutz, W. Männer, H.-G. Moser, R. Richter, A. Rosado-Schlosser, S. Schael, R. Settles, H. Seywerd, R. St. Denis, W. Wiedenmann, G. Wolf

Max-Planck-Institut für Physik, Werner-Heisenberg-Institut, 80805 München, Fed. Rep. of Germany[16]

J. Boucrot, O. Callot, A. Cordier, M. Davier, L. Duflot, J.-F. Grivaz, Ph. Heusse, A. Höcker, M. Jacquet, D.W. Kim,[19] F. Le Diberder, J. Lefrançois, A.-M. Lutz, I. Nikolic, H.J. Park,[19] I.C. Park,[19] M.-H. Schune, S. Simion, J.-J. Veillet, I. Videau, D. Zerwas

Laboratoire de l'Accélérateur Linéaire, Université de Paris-Sud, IN^{2}P^3-CNRS, 91405 Orsay Cedex, France

P. Azzurri, G. Bagliesi, G. Batignani, S. Bettarini, C. Bozzi, G. Calderini, M. Carpinelli, M.A. Ciocci, V. Ciulli, R. Dell'Orso, R. Fantechi, I. Ferrante, A. Giassi, A. Gregorio, F. Ligabue, A. Lusiani, P.S. Marrocchesi, A. Messineo, G. Rizzo, G. Sanguinetti, A. Sciabà, P. Spagnolo, J. Steinberger, R. Tenchini, G. Tonelli,[26] C. Vannini, P.G. Verdini, J. Walsh

Dipartimento di Fisica dell'Università, INFN Sezione di Pisa, e Scuola Normale Superiore, 56010 Pisa, Italy

G.A. Blair, L.M. Bryant, F. Cerutti, J.T. Chambers, Y. Gao, M.G. Green, T. Medcalf, P. Perrodo, J.A. Strong, J.H. von Wimmersperg-Toeller

Department of Physics, Royal Holloway & Bedford New College, University of London, Surrey TW20 OEX, United Kingdom[10]

D.R. Botterill, R.W. Clifft, T.R. Edgecock, S. Haywood, P. Maley, P.R. Norton, J.C. Thompson, A.E. Wright

Particle Physics Dept., Rutherford Appleton Laboratory, Chilton, Didcot, Oxon OX11 OQX, United Kingdom[10]

B. Bloch-Devaux, P. Colas, S. Emery, W. Kozanecki, E. Lançon, M.C. Lemaire, E. Locci, B. Marx, P. Perez, J. Rander, J.-F. Renardy, A. Roussarie, J.-P. Schuller, J. Schwindling, A. Trabelsi, B. Vallage

CEA, DAPNIA/Service de Physique des Particules, CE-Saclay, 91191 Gif-sur-Yvette Cedex, France[17]

S.N. Black, J.H. Dann, R.P. Johnson, H.Y. Kim, A.M. Litke, M.A. McNeil, G. Taylor

Institute for Particle Physics, University of California at Santa Cruz, Santa Cruz, CA 95064, USA[22]

C.N. Booth, R. Boswell, C.A.J. Brew, S. Cartwright, F. Combley, A. Koksal, M. Letho, W.M. Newton, J. Reeve, L.F. Thompson

Department of Physics, University of Sheffield, Sheffield S3 7RH, United Kingdom[10]

A. Böhrer, S. Brandt, V. Büscher, G. Cowan, C. Grupen, G. Lutters, P. Saraiva, L. Smolik, F. Stephan,

Fachbereich Physik, Universität Siegen, 57068 Siegen, Fed. Rep. of Germany[16]

M. Aleppo,[20] M. Apollonio, L. Bosisio, R. Della Marina, G. Giannini, B. Gobbo, G. Musolino, F. Ragusa[20,21]

Dipartimento di Fisica, Università di Trieste e INFN Sezione di Trieste, 34127 Trieste, Italy

J. Putz, J. Rothberg, S. Wasserbaech, R.W. Williams

Experimental Elementary Particle Physics, University of Washington, WA 98195 Seattle, U.S.A.

S.R. Armstrong, L. Bellantoni,[23] P. Elmer, Z. Feng, D.P.S. Ferguson, Y.S. Gao, S. González, J. Grahl, T.C. Greening, J.L. Harton,[27] O.J. Hayes, H. Hu, P.A. McNamara III, J.M. Nachtman, W. Orejudos, Y.B. Pan, Y. Saadi, M. Schmitt, I.J. Scott, V. Sharma,[25] J.D. Turk, A.M. Walsh, Sau Lan Wu, X. Wu, J.M. Yamartino, M. Zheng, G. Zobernig

Department of Physics, University of Wisconsin, Madison, WI 53706, USA[11]

---

[1] Now at DESY, Hamburg, Germany.
[2] Supported by Dirección General de Investigación Científica y Técnica, Spain.
[3] Now at Dipartimento di Fisica, Università di Lecce, 73100 Lecce, Italy.
[4] Also Istituto di Fisica Generale, Università di Torino, Torino, Italy.
[5] Also Istituto di Cosmo-Geofisica del C.N.R., Torino, Italy.
[6] Supported by the Commission of the European Communities, contract ERBCHBICT941234.
[7] Supported by CICYT, Spain.
[8] Supported by the National Science Foundation of China.
[9] Supported by the Danish Natural Science Research Council.
[10] Supported by the UK Particle Physics and Astronomy Research Council.
[11] Supported by the US Department of Energy, grant DE-FG0295-ER40896.
[12] Also at Supercomputations Research Institute, Florida State University, Tallahassee, U.S.A.
[13] Supported by the US Department of Energy, contract DE-FG05-92ER40742.
[14] Supported by the US Department of Energy, contract DE-FC05-85ER250000.
[15] Permanent address: Universitat de Barcelona, 08208 Barcelona, Spain.
[16] Supported by the Bundesministerium für Forschung und Technologie, Fed. Rep. of Germany.
[17] Supported by the Direction des Sciences de la Matière, C.E.A.
[18] Supported by Fonds zur Förderung der wissenschaftlichen Forschung, Austria.
[19] Permanent address: Kangnung National University, Kangnung, Korea.
[20] Now at Dipartimento di Fisica, Università di Milano, Milano, Italy.
[21] Also at CERN, 1211 Geneva 23, Switzerland.
[22] Supported by the US Department of Energy, grant DE-FG03-92ER40689.
[23] Now at Fermi National Accelerator Laboratory, Batavia, IL 60510, USA.
[24] Now at Max-Plank-Institüt für Kernphysik, Heidelberg, Germany.
[25] Now at University of California at San Diego, La Jolla, CA 92093, USA.
[26] Also at Istituto di Matematica e Fisica, Università di Sassari, Sassari, Italy.
[27] Now at Colorado State University, Fort Collins, CO 80523, USA.

1 Introduction

The major phenomenological consequence of supersymmetric theories [1] is that the spectrum of physical states is doubled: each matter fermion has two spin-0 partners (one for each helicity state); each massless gauge boson has a spin-1/2 partner; and each massive gauge boson, together with a Higgs boson, has two spin-1/2 partners. Since none of these new states has been observed degenerate in mass with its ordinary partner, supersymmetry must be broken. When supersymmetry is broken, not only is the mass degeneracy between ordinary and supersymmetric particles lifted, but also mixing occurs among the electroweak eigenstates. In particular, the partners of the W and charged Higgs bosons mix to form "charginos", while the partners of the photon, of the Z and of the neutral Higgs bosons mix to form "neutralinos". To preserve one of the most attractive features of supersymmetry, namely that it offers a solution to the naturalness problem of the Higgs sector, the mass splitting between ordinary and supersymmetric particles should not be too large, less than a TeV/c^2 or so, and some of the new states are even expected to have masses below 100 GeV/c^2 [2]. Hence the great interest of any energy increase at LEP, CERN's large e^+e^- collider.

From 1989 to the autumn of 1995, LEP had been operated at centre-of-mass energies close to the Z peak. It is expected that the threshold for W-pair production will be passed in 1996, thanks to a major upgrade of the accelerating system involving the installation of a large number of superconducting cavities. An intermediate step took place during the last month of operation in 1995, allowing centre-of-mass energies up to 136 GeV to be explored. Integrated luminosities of 2.8 and 2.9 pb^{-1} were accumulated by the ALEPH detector at 130 and 136 GeV, respectively, with all the detector subsystems fully operational.

This letter reports searches for supersymmetric particles performed with this data sample. R-parity, a new quantum number which distinguishes ordinary and supersymmetric particles [3], is assumed to be conserved, which implies that supersymmetric particles are produced in pairs and that the lightest one, the LSP, is stable. Unless explicitly stated, it is also assumed that the lightest of the neutralinos, χ, is the LSP. It is weakly interacting, which is at the origin of the characteristic experimental signature of supersymmetry: missing energy. Since $e^+e^- \to \chi\chi$ leads to invisible final states, the reactions which have been considered are:

- Slepton pair production $e^+e^- \to \tilde{\ell}^+\tilde{\ell}^-$;
- Chargino pair production $e^+e^- \to \chi^+\chi^-$;
- Associated neutralino production $e^+e^- \to \chi\chi'$;
- Stop pair production $e^+e^- \to \tilde{t}\,\bar{\tilde{t}}$.

The sleptons (selectrons, smuons, and staus) are the scalar partners of the ordinary leptons. They are called "right" or "left" sleptons, depending on the helicity state to which they are associated. Similarly, the scalar partners of the ordinary quarks are the squarks,

and those of the neutrinos are the sneutrinos. The lighter of the two partners of the top quark is called the stop. Pair production of sneutrinos has not been considered since it leads to invisible final states ($\tilde{\nu} \to \nu\chi$). Little mixing is expected to occur among right and left sleptons or squarks, except possibly in the stop sector because of the large top quark mass [4]. For squarks other than the stop, the mass limits from $p\overline{p}$ colliders [5] leave no room for searches in e^+e^- collisions at LEP energies.

In the following, the Minimal Supersymmetric extension of the Standard Model [6], the MSSM, is used as a reference model, although the analyses reported here are valid in a broader framework. In the MSSM, only a few parameters are needed to specify all supersymmetric particle masses and couplings, among which a supersymmetric Higgs mass term, μ, and a supersymmetry breaking mass term, M_2, associated with the $SU(2)_L$ gauge group. The unification condition, $M_1 = \frac{5}{3}\tan^2\theta_W M_2$, is assumed, where M_1 is the mass term associated with the $U(1)_Y$ group. The charginos and neutralinos are "higgsino-like" when $|\mu| \ll M_2$, and "gaugino-like" in the opposite case. The ratio of the vacuum expectation values of the two Higgs doublets is denoted $\tan\beta$.

1.1 Supersymmetric particle production and decay mechanisms

Slepton pair production, $e^+e^- \to \tilde{\ell}^+\tilde{\ell}^-$, is mediated by s-channel Z and photon exchange and, in the case of selectrons, by t-channel neutralino exchange. The latter contribution substantially enhances the selectron production cross-section when the lightest neutralino is predominantly gaugino-like. Conservative limits are set by considering only right sleptons, as their production cross-section is lower than that of left sleptons. Moreover, in the MSSM, the slepton masses receive radiative corrections *via* gaugino loops which render the left sleptons heavier than the right ones. The production cross-section for a pair of right smuons of mass 50 GeV/c^2 is half a picobarn at 136 GeV. Right sleptons decay into their ordinary partner and a neutralino, $\tilde{\ell} \to \ell\chi$.

Chargino pair production, $e^+e^- \to \chi^+\chi^-$, is mediated by s-channel Z and photon exchange, and by t-channel sneutrino exchange. These two contributions interfere destructively, an effect which is most pronounced when the sneutrino is light and when the chargino is predominantly gaugino-like. When sneutrino exchange can be ignored, *i.e* if sneutrinos are very massive or if the chargino is higgsino-like, the production cross-section at 136 GeV ranges from 5.5 to 18 pb for a 60 GeV/c^2 mass chargino, depending on its field content. Charginos decay *via* virtual W exchange into $\chi\,\mathrm{f}\overline{\mathrm{f'}}$, where f and f' belong to the same weak isodoublet (*e.g.* $e^+\nu_e$ or $u\overline{d}$). Except for possible phase space suppression when the $\chi^\pm - \chi$ mass difference is small, the decay branching ratios into each of the lepton flavours are 11%, and 67% into hadronic final states. Virtual slepton and squark exchanges in the $\chi^\pm$ decay lead to the same final states, but their contribution may modify the above branching ratios. In the MSSM, this will usually increase the leptonic branching ratios since sleptons are expected to be substantially lighter than squarks. In the extreme situation where sneutrinos are lighter than the chargino, the two-body decays $\chi^+ \to \ell\tilde{\nu}$ become dominant.

The second lightest neutralino, χ', could be produced together with the lightest one in the reaction $e^+e^- \to \chi\chi'$, mediated by s-channel Z exchange, and by t-channel selectron exchange. In contrast to the cases of slepton and chargino production, the couplings involved in neutralino production are very strongly model dependent. For $m_\chi + m_{\chi'} = 120$ GeV/c^2, a cross-section as large as 5 pb can be reached at 136 GeV for higgsino-like neutralinos. The subsequent $\chi' \to \chi f\bar{f}$ decay proceeds *via* virtual Z exchange, with typical branching ratios of 70% into hadrons, 10% into charged leptons and 20% into neutrinos. Here too, virtual slepton and squark exchanges may contribute, normally enhancing the leptonic branching ratios. Again, in the extreme situation where sneutrinos are lighter than the χ', the two-body decays $\chi' \to \bar{\nu}\tilde{\nu}$ become dominant, and the final state is invisible.

Stop pair production, $e^+e^- \to \tilde{t}\,\bar{\tilde{t}}$, is mediated by s-channel Z and photon exchange. The coupling of the stop to the Z depends on the value of the mixing angle θ_t; it vanishes for $\theta_t \sim 0.98$ rad, and is maximal for $\cos\theta_t = 1$. In this last case, the production cross-section for a pair of 60 GeV/c^2 mass stops is 0.65 pb at 136 GeV. With the $\tilde{t} \to \chi t$ and $\tilde{t} \to \chi^+ b$ decay channels kinematically forbidden, the dominant stop decay mode is the one-loop process $\tilde{t} \to \chi c$.

1.2 Signal and background simulations

To design the selection criteria and evaluate their efficiencies, various Monte Carlo generators for the supersymmetric signals have been used. They are essentially identical to those used in the former ALEPH searches for supersymmetric particles [7, 8], except in the case of charginos where the `SUSYGEN` program [9] has been used. In all cases, initial state radiation is taken into account, and, in addition, photon radiation from the final state leptons has been implemented according to the `PHOTOS` package [10]. Given the many possible channels and parameters, full simulations of the detector response were performed only for a restricted number of points, in particular close to the boundaries of the sensitivity domains, and a fast but nevertheless sufficiently accurate simulation program was used to interpolate between those points.

Monte Carlo samples corresponding to integrated luminosities at least twenty times as large as that of the data have been fully simulated for all major standard background reactions. These include the annihilation processes $e^+e^- \to f\bar{f}(\gamma)$, of which about two thirds are due to the radiative return to the Z (*i.e.* $e^+e^- \to Z\gamma$), the two-photon scattering processes $\gamma\gamma \to f\bar{f}$, and the various other processes leading to four-fermion final states. In this last case, the main contributions arise from the reactions $e^+e^- \to WW$, $e^+e^- \to ZZ$, $e^+e^- \to We\nu$ and $e^+e^- \to Zee$, where the W or Z bosons may be off-shell, and where Z stands for a Z boson or a virtual photon. All processes were generated using the `PYTHIA` package [11], except for W-pair production and for gamma-gamma scattering where the `LPWW02` [12] and `PHOT02` [13] programs were used, respectively. In addition, the four-fermion final state generation has been verified using the `FERMISV` program [14], especially to check the background coming from the $f\bar{f}\nu\bar{\nu}$ final states.

1.3 The ALEPH detector

A thorough description of the ALEPH detector can be found in Ref. [15], and an account of its performance as well as a description of the standard analysis algorithms in Ref. [16].

Briefly, the tracking system consists of a newly installed silicon vertex detector, a cylindrical drift chamber and a large time projection chamber (TPC), all immersed in a 1.5 T magnetic field provided by a superconducting solenoidal coil. Between the TPC and the coil, a highly granular electromagnetic calorimeter is used to identify electrons and photons and to measure their energy. Complemented by luminosity calorimeters, the coverage is hermetic down to 24 mrad from the beam axis. The iron return yoke is instrumented to provide a measurement of the hadronic energy and, together with external chambers, muon identification.

All this information is combined in an energy flow algorithm which supplies the analysis programs with a list of "particles", categorized as photons, as neutral hadrons and as charged particles, of which some are identified electrons and muons.

For the processes of interest here, the relevant trigger conditions were found to be highly redundant and fully efficient for the simulated signal events surviving the selection criteria described in the next section.

2 Topological searches

Various searches have been designed in order to be sensitive to the different topologies which could arise from the production of sleptons, charginos, neutralinos or stops. Each analysis has been optimized on Monte Carlo samples in order to obtain maximal efficiency for a total expected background of ~ 0.2 pb.

Slepton pair production leads to final states consisting of a pair of leptons of the same flavour, with missing energy and momentum taken away by the two χs. A search for acoplanar lepton pairs has therefore been designed.

Depending on whether both, only one, or neither of the produced charginos decay leptonically, the final state topologies arising from chargino pair production are:

- a pair of leptons, not necessarily of the same flavour, with missing energy taken away by the χs (and also by the decay neutrinos). The search for acoplanar lepton pairs mentioned above copes with this topology.
- a lepton and two hadronic jets, with missing energy taken away by the χs (and by the neutrino from the leptonic decay).
- four hadronic jets, with missing energy taken away by the χs.

Searches for isolated leptons in hadronic environments and for hadronic events with missing energy have been designed for these last two topologies.

Associated $\chi\chi'$ production followed by $\chi' \to \chi\, f\bar{f}$ leads to visible final states consisting of a lepton pair or of two hadronic jets with missing energy. The search for acoplanar lepton pairs was found to be sufficiently efficient. However, the search for hadronic events with missing energy, designed for chargino pairs, had to be supplemented with a dedicated analysis: even though no explicit jet reconstruction is performed, the topologies arising from two and four-jet final states turn out to be sufficiently different that two sets of search criteria are required.

Stop pair production followed by $\tilde{t} \to \chi\, c$ leads to a pair of acoplanar hadronic jets. The criteria designed for the neutralino search were found to be well suited to that case too.

In the following subsections, these various searches are described, and their efficiencies summarized together with the background levels expected.

2.1 Search for acoplanar lepton pairs

To select acoplanar lepton pairs arising from slepton or from chargino production, the following criteria have been applied.

There should be exactly two or four good charged particle tracks, with no explicit lepton identification being required. Such "good tracks" originate from within a cylinder of 2 cm radius and 20 cm length, coaxial with the beam axis and centered on the nominal interaction point. The polar angles of these tracks, measured with respect to the beam axis, should be larger than 18.2°. The total electric charge should be zero. If there are four tracks, at least one triplet of tracks should have a mass smaller than 1.5 GeV/c^2; the triplet with the smallest mass, considered as resulting from a τ decay, is treated as a single particle. Such triplets and the remaining charged particles are hereafter called "leptons" for simplicity.

Both leptons should have momenta larger than 0.7 GeV/c, and the event visible mass should exceed 4 GeV/c^2. The acoplanarity angle of the two leptons should be smaller than 170°, which removes most of the events from the reaction $e^+e^- \to \ell^+\ell^-(\gamma)$. The acoplanarity angle is the angle between the projections of the lepton momenta onto a plane perpendicular to the beam axis. The background from $e^+e^- \to \ell^+\ell^-\gamma$, with the photon detected, is eliminated by a "photon veto". An event is rejected if it contains a photon with energy above 1 GeV, provided that this photon does not make an angle smaller than 10° with either of the two leptons, and that its invariant mass with each of the two leptons is larger than 2 GeV/c^2. These restrictions avoid vetoing τ decays.

To eliminate the background from tagged two-photon processes, it is required that no energy be detected within 12° of the beam axis. The inefficiency, due to beam related background and to electronic noise, introduced by this requirement and by the above described photon veto, was measured to be less than 0.5%, using events triggered at random beam crossings. The background from untagged two-photon processes is drastically reduced by the requirement that the total momentum transverse to the beam axis should exceed $2.5\%\sqrt{s}$. Some of the background from $\gamma\gamma \to \tau^+\tau^-$ however survives at

this stage because of the additional transverse momentum carried away by the τ-decay neutrinos. To eliminate this background, the following procedure is applied: the lepton momenta are projected onto a plane perpendicular to the beam axis, and a 2d-thrust axis is computed from these projections; the scalar sum ρ of the transverse components of the 2d-lepton momenta, measured with respect to the 2d-thrust axis, is required to be larger than 2 GeV/c. The effectiveness of this cut is demonstrated in Fig. 1a.

2.2 Search for hadronic events with isolated leptons

To search for hadronic events containing an isolated lepton arising from the production of a chargino pair, a preselection is first applied. A minimum of four good tracks and a visible mass of at least 4 GeV/c^2 are required. No photon with an energy in excess of 10 GeV and isolated in a cone of half-angle 30° should be detected; the aim of this criterion is to eliminate the background from $e^+e^- \to f\bar{f}\gamma$, dominated by the radiative return to the Z, with the photon emitted at large angle with respect to the beam axis. Two sets of search criteria were designed to cope with the possibilities that the mass difference between the chargino and the neutralino may be large or small.

For large mass differences, a minimum of five charged tracks is required. To reduce the large background from the reaction $e^+e^- \to q\overline{q}(\gamma)$, an acoplanarity angle smaller than 175° is required. Here, the acoplanarity is calculated from the directions of the momenta of the two event hemispheres, defined by a plane perpendicular to the thrust axis. In addition, the direction of the missing momentum should not point within 18.2° of the beam axis. The background from two-photon interactions is largely eliminated by the requirement that the missing transverse momentum should exceed $5\%\sqrt{s}$. At least one particle identified as an electron or a muon must be found with a momentum larger than 5 GeV/c, and a cone of half-angle 30° around its direction must contain less than 5 GeV of additional energy. The electron identification relies on the transverse and longitudinal profiles of the associated shower in the electromagnetic calorimeter; the muon identification makes use of the penetration and of the transverse profile in the hadronic calorimeter, and of the muon chamber information [16]. The distribution of the highest lepton momentum is shown in Fig. 1b. The few events expected to remain at this point from singly tagged two-photon interactions are eliminated by the requirement that the lepton energy should be smaller than $30\%\sqrt{s}$. Finally, the small background from WW* final states is eliminated by the requirement that the visible mass should be smaller than 60 GeV/c^2, once the lepton has been excluded.

For small mass differences, the main background arises from two-photon interactions. Therefore, it is required that the missing transverse momentum exceed 2 GeV/c, that the angle of the thrust axis with respect to the beam be larger than 25.8°, and that no energy be detected within 12° of the beam axis. In addition, the projected acoplanarity angle should be smaller than 135°. The projected acoplanarity angle is obtained by first projecting the event onto a plane perpendicular to the beam axis, then calculating the thrust axis and dividing the event into two hemispheres by a plane perpendicular to that thrust axis. A lepton, electron or muon, must be found with a momentum larger than

2 GeV/c, and with less than 1 GeV of additional energy in a cone of half-angle 30° around its direction.

2.3 Search for hadronic events with missing energy

After the same preselection as above, two sets of criteria are designed to search for hadronic events originating from chargino pairs, optimized for large and for small mass differences between the chargino and the neutralino. In both cases, however, the event thrust is required to be smaller than 0.9, which eliminates back-to-back fermion pairs, and the transverse imbalance, defined as the ratio of the missing transverse momentum to the visible energy, should exceed 20%. This latter requirement eliminates a large fraction of the background from $e^+e^- \to f\bar{f}(\gamma)$ and from two-photon processes.

For large mass differences, a minimum of seven charged tracks is required. The acoplanarity angle should be smaller than 175°, the direction of the missing momentum should not point within 18.2° of the beam axis, and the transverse momentum should exceed $5\%\sqrt{s}$. It is further required that an energy E_w smaller than $10\%\sqrt{s}$ should be found in an azimuthal wedge of half-angle 30° drawn around the direction of the missing transverse momentum. Such a wedge copes well with situations in which the direction of the missing momentum is spoilt by undetected initial state radiation along the beam axis, and is preferred to a simple cone around the direction of the missing momentum. The distribution of E_w is shown in Fig. 1c. Because of the potentially large background due to radiative returns to the Z followed by $Z \to b\overline{b}(g)$ with b or $\bar{b}$-semileptonic decays, the following procedure is applied: the energy of the radiative photon, assumed to be emitted along the beam direction, and the momentum of the missing neutrino are calculated from energy and momentum conservation; the direction of the missing neutrino is required to point well within the detector, *i.e.* beyond 18.2° from the beam axis; if the energy of the radiated photon exceeds 35 GeV, as expected for a radiative return to the Z, the upper limit on E_w is then lowered to 9 GeV. At this level, the only significant backgrounds left come from the WW^* and $We\nu$ final states. Their contributions are strongly reduced by the following requirements, applied only if the visible mass exceeds 70 GeV/c^2: *i)* there should be no lepton, electron or muon, with an energy larger than 5 GeV; *ii)* the event should not resemble a boosted two-jet system; to this end, the quadratic mean of the two inverse hemisphere boosts ($\sqrt{((m_1/E_1)^2+(m_2/E_2)^2)/2}$, with $m_{1,2}$ and $E_{1,2}$ the two hemisphere masses and energies) is required to be larger than 0.45.

For small mass differences, where the main backgrounds come from two-photon interactions, the projected acoplanarity angle is required not to exceed 135°, and even 90° if the event visible mass is smaller than 7 GeV/c^2. In addition, the angle of the thrust axis with the beam should be larger than 45°, and no energy should be detected within 12° of the beam axis. The same reconstruction procedure as in the case of large mass differences is then applied, but now interpreting the directions of the radiative photon and of the decay neutrino as those of untagged electrons in two-photon processes, one of which assumed along the beam direction. The cosine of the angle of the "neutrino" direction with the beam axis is required to be smaller than 0.999, in which case it should be detected in the luminosity calorimeters. Tagged two-photon interactions are eliminated

by the requirement that no electron should be found with an energy larger than $30\%\sqrt{s}$. Finally, the missing momentum should be isolated, which is ensured by the requirement that E_w be smaller than 1 GeV.

2.4 Search for acoplanar jets

To search for acoplanar jets from hadronic neutralino decays, the same preselection is again applied, and also the same transverse imbalance requirement of at least 20%; but the cut on the event thrust is softened to 0.95. The projected acoplanarity angle, the distribution of which is shown in Fig. 1d, is required to be smaller than 150°. The missing transverse momentum should exceed $3.75\%\sqrt{s}$ and should be isolated with E_w smaller than $10\%\sqrt{s}$. The event visible mass should be smaller than $40\%\sqrt{s}$. This last requirement is guided by the MSSM where neutralino production occurs with a substantial cross-section only when the mass difference between the two lightest neutralinos is small or moderate.

Two sets of selection criteria are applied at this point, optimized for larger and for smaller mass differences between the second lightest and the lightest neutralinos. For larger mass differences, a minimum of seven charged tracks is required, the missing transverse momentum should exceed $5\%\sqrt{s}$ and the missing momentum should not point within 25.8° of the beam axis. For smaller mass differences, the projected acoplanarity angle should not exceed 135°, and even 90° if the event visible mass is smaller than 7 GeV/c^2, no energy should be detected within 12° of the beam axis, and the requirement on the isolation of the missing momentum is tightened to a maximum of 1 GeV for E_w.

2.5 Background levels and efficiencies

The expected background from all these topological searches combined is 0.22 pb, of which 0.10 pb come from $e^+e^- \to f\bar{f}(\gamma)$ and from two-photon interactions, and 0.12 pb come from other processes leading to four-fermion final states. This corresponds to 1.3 events expected in the 5.7 pb^{-1} of data. No candidate events were selected.

The selection efficiencies for 60 GeV/c^2 mass sleptons produced at a centre-of-mass energy of 133 GeV are displayed in Table 1 for three values of the LSP mass. These efficiencies can reach values as high as 75%, but they are substantially lower when the mass difference between the slepton and the LSP becomes small. As expected, the efficiencies are smaller for staus than for selectrons or smuons.

The selection efficiencies at 133 GeV for 65 GeV/c^2 mass charginos are displayed in Table 2 for the different possible final states resulting from three-body chargino decays and for three values of the LSP mass. The overall efficiencies are also given for the combination where these various final states are weighted as expected from W-exchange dominance in chargino decays. Overall efficiencies well in excess of 70% are obtained in the most favourable cases, and still as high as 17% when the $\chi^+ - \chi$ mass difference is

only 5 GeV/c^2. In the case where sneutrinos are lighter than the chargino, the two body decays $\chi^+ \to \ell\tilde{\nu}$ dominate, leading to even larger efficiencies.

Typical efficiencies at 133 GeV for $e^+e^- \to \chi\chi'$ are 50% for χ' and χ masses of 80 and 45 GeV/c^2, and 14% for masses of 70 and 60 GeV/c^2. Here, Z-exchange dominance in χ' decays is assumed, leading to invisible final states in $\sim 20\%$ of the cases.

For 60 GeV/c^2 mass stops pair produced at 133 GeV, the selection efficiency is 64% for $m_\chi = 30$ GeV/c^2.

3 Results

With no events found in 2.8 pb^{-1} at 130 GeV and in 2.9 pb^{-1} at 136 GeV, constraints on the masses of various supersymmetric particles and limits on their production cross-sections can be derived. In all cases, the numbers of events expected have been conservatively reduced by the systematic errors thereon. These systematic uncertainties ($\sim 3\%$) are mostly due to the limited Monte Carlo statistics, with small additional contributions from the luminosity measurement, from the lepton identification efficiencies, from the energy calibrations and from the hadronization models.

3.1 Limits on sleptons

For right smuons and staus, the production cross-section depends only on the mass of the produced slepton. Mass lower limits of 44 and 38 GeV/c^2 can be derived for low χ masses, which does not improve on the results obtained at LEP1 [7].

For the right selectron, $\tilde{e}_R$, the production cross-section also depends on the mass and on the field content of the neutralinos which are exchanged in the t-channel. As a result, interesting limits can be obtained when these contributions are enhanced, which occurs in the "deep gaugino" region. In the MSSM, this corresponds to $|\mu| \gg M_2$. The exclusion domain shown in Fig. 2 has been derived in this context, with $\mu = 1$ TeV/c^2 and $\tan\beta = 2$. The dependence on $\tan\beta$ is very weak.

For $m_\chi = 0$, the 95% C.L. mass lower limit is 59 GeV/c^2. At the 90 % C.L., and assuming mass degeneracy of the left and right selectrons, the limit becomes 63 GeV/c^2. This is significantly lower than the 90% C.L. lower limit of 73 GeV/c^2 achieved for mass degenerate selectrons by a combination of single photon searches at lower energy e^+e^- machines [17]. Besides, χ masses smaller than 35 GeV/c^2 correspond, for the above value of μ and $\tan\beta$, to chargino masses smaller than 67.8 GeV/c^2 which, anticipating the results of the next subsection, are excluded.

For $m_\chi > 35$ GeV/c^2, the mass splitting between left and right selectrons is such that only $\tilde{e}_R$ pair production is kinematically allowed. The 95% C.L. lower limit on the right selectron mass is 53 GeV/c^2 for $m_\chi = 35$ GeV/c^2. If equal selectron, smuon and stau

masses are assumed, the limit on the common right slepton mass improves to 57 GeV/c^2. For such large χ mass values, there are no limits from the single photon searches.

3.2 Limits on charginos and neutralinos

3.2.1 Cross-section limits

The topological searches described in Section 2 provide a good acceptance for charginos and neutralinos with little dependence on the details of the model. For example, the overall acceptance of 74% for charginos, with a chargino-neutralino mass difference of 35 GeV/c^2, varies by less than 4% as the branching ratio for $\chi^+ \to \ell\nu\chi$ varies from 0% to 60%, and remains at the level of 59% when this branching ratio is 100% (Table 2). The acceptance depends primarily on the mass difference $\Delta m = m_{\chi^+} - m_\chi$ with only a slight variation with m_{χ^+}.

The data recorded at the two centre-of-mass energies lead to two upper limits on the signal cross-section. These can be combined if one assumes a simple β dependence of the cross-section, valid for pure gauginos for instance. To this end, an effective luminosity is defined:

$$\mathcal{L}_{\text{eff}} = \frac{\beta(m_{\chi^+}, \sqrt{s} = 130 \text{ GeV})}{\beta(m_{\chi^+}, \sqrt{s} = 136 \text{ GeV})} \cdot \mathcal{L}_{130} + \mathcal{L}_{136}.$$

Here, $\beta(m_{\chi^+}, \sqrt{s})$ is the chargino velocity, and $\mathcal{L}_{130}$ and $\mathcal{L}_{136}$ are the integrated luminosities for $\sqrt{s} = 130$ and 136 GeV. With this definition of the luminosity, an upper limit on the cross-section is derived, valid for $\sqrt{s} = 136$ GeV. It is displayed in Fig. 3 as a function of the chargino and neutralino masses, assuming W* exchange dominance in chargino decays.

Production cross-sections above 3 pb at $\sqrt{s} = 136$ GeV are excluded at the 95% C.L. for $m_{\chi^+} < 64$ GeV/c^2 and $\Delta m > 5$ GeV/c^2. For $64 < m_{\chi^+} < 67.8$ GeV/c^2, the same limit holds when $\Delta m > 10$ GeV/c^2, or at 5 pb for $\Delta m > 5$ GeV/c^2. These cross-section limits are to be compared with the expectations of 5.5 to 18 pb mentioned in Section 1.1. In the MSSM, the neutralino mass is typically half the chargino mass in the deep gaugino region. In that case, the upper limit on the cross-section is less than 1 pb up to $m_{\chi^+} = 64$ GeV/c^2. If sneutrinos are lighter than the chargino, the two-body leptonic decays $\chi^+ \to \ell\tilde{\nu}$ dominate and the limits presented in Fig. 3, reinterpreting m_χ as the sneutrino mass, are valid but conservative since the acceptance is higher.

A similar approach can be used for associated neutralino production. When deriving limits in the $(m_\chi, m_{\chi'})$ plane, Z* exchange dominance in χ' decays has been assumed for calculating the branching ratios. Such Z* exchange dominance is characteristic of the deep higgsino region. The cross-section limits are shown in Fig. 4. In general, cross-sections larger than 5 pb are excluded when $m_{\chi'} - m_\chi > 10$ GeV/c^2.

3.2.2 Interpretation in the MSSM

In the MSSM, the masses and production cross-sections for charginos and neutralinos depend firstly on M_2, μ, and $\tan\beta$, and secondly on the masses of the sleptons exchanged in the t-channel (sneutrinos for charginos, selectrons for neutralinos). Consequently, the experimental results depicted in Figs. 3 and 4 can be translated into excluded regions in the MSSM parameter space, as shown in Fig. 5. The cross-sections were calculated according to Ref. [18], including initial state radiation which reduces somewhat the Born cross-sections, for instance by 15% for $m_{\chi^+} = 62$ GeV/c^2 at a centre-of-mass energy of 136 GeV. Two values of $\tan\beta$, 1.41 and 35, are considered, representative of the low and high $\tan\beta$ regimes favoured by the large top quark mass in the framework of supersymmetric grand unified theories [19]. The slepton masses are set to high values ($m_{\tilde{\ell}} = 500$ GeV/c^2). The negative result from the topological searches interpreted in terms of chargino production is shown as a shaded area. If instead neutralino production is considered, the hatched region is excluded. In the derivation of these results, all chargino and neutralino cascade decays have been explicitly taken into account, as implemented in the `SUSYGEN` generator [9]. In the higgsino region, the boundaries in $|\mu|$ have been extended by about 20 GeV/c^2 (for $M_2 = 500$ GeV/c^2) with respect to LEP1 [7, 20], and, in the gaugino region, the boundaries in M_2 have been extended by about 22 GeV/c^2 (for $|\mu| = 500$ GeV/c^2).

The sensitivity of the chargino production cross-section to the sneutrino mass is greatest in the gaugino region. The lower limit on the chargino mass as a function of μ in the gaugino region is shown in Fig. 6. Because Δm, and therefore the acceptance, are large in that case, the exclusion extends to within a few hundred MeV of the kinematic limit when $m_{\tilde{\nu}} > 200$ GeV/c^2 or so. For lighter sneutrinos the destructive interference between t-channel and s-channel diagrams weakens the limit somewhat, as shown in the lower plot for a specific value of μ. For moderate values of μ the limit depends on $\tan\beta$, as shown. For even lower sneutrino masses, the two-body decay $\chi^+ \to \ell\tilde{\nu}$ becomes kinematically allowed, in which case it is dominant. As the mass difference $m_{\chi^+} - m_{\tilde{\nu}}$ becomes smaller, the leptons become softer and the acceptance lower, forbidding at some point any chargino limit to be obtained.

The lower limit on the chargino mass in the higgsino region is shown as a shaded region in Fig. 7, for $\tan\beta = 1.41$. The decrease of the limit for large M_2 values is related to a corresponding decrease of Δm, and therefore of the acceptance. The result for $\tan\beta = 35$ is very similar. The limit on the second lightest neutralino mass is shown as the upper lines (solid for $\tan\beta = 1.41$, dashed for $\tan\beta = 35$). The lower lines are the limits on the chargino mass inferred from the neutralino search; for small $\tan\beta$ they extend the limit for $\mu < 0$. In this plot M_2 has been signed by μ for the purposes of depiction only: the results shown for $M_2 < 0$ are obtained taking $M_2 > 0$ and finding the limit for $\mu < 0$. Throughout the higgsino region with $M_2 < 1$ TeV, the limits $m_{\chi^+} > 63$ GeV/c^2 and $m_{\chi'} > 68$ GeV/c^2 hold for $\tan\beta = 1.41$. There is little dependence of these limits on $\tan\beta$.

3.3 Limits on stops

The stop production cross-section depends on the mixing angle θ_t. When the stop coupling to the Z vanishes (*i.e.* for $\theta_t \sim 0.98$ rad), there is no improvement on the limits obtained at LEP1 [8, 21]. For a purely right stop (*i.e.* for $\cos\theta_t = 0$), the gain with respect to LEP1 is moderate: $m_{\tilde{t}} < 48$ GeV/c^2 is excluded at the 95% C.L. for $m_\chi \sim 30$ GeV/c^2. In the theoretically unlikely case where the lightest mass eigenstate is a purely left stop (*i.e.* for $\cos\theta_t = 1$), $m_{\tilde{t}} < 57$ GeV/c^2 is excluded at the 95% C.L. for $m_\chi < 43$ GeV/c^2.

4 Conclusions

In a data sample of 5.7 pb^{-1} collected by the ALEPH detector at LEP at centre-of-mass energies of 130 and 136 GeV, searches for signals of supersymmetric particle production have been performed in the following topologies:

- acoplanar lepton pairs,
- hadronic events with isolated leptons,
- hadronic events with missing energy,
- acoplanar jets.

No candidate events were found, from which limits on supersymmetric particle masses and on their production cross-sections have been derived. The results are summarized in Figs. 2 to 7. In particular, the following mass lower limits are set at the 95% confidence level:

- 53 GeV/c^2 for scalar electrons when the lightest neutralino, χ, is gaugino-like and has a mass smaller than 35 GeV/c^2;
- 67.8 GeV/c^2 for gaugino-like charginos, when the scalar neutrino mass is larger than 200 GeV/c^2;
- 65 GeV/c^2 for higgsino-like charginos, when the mass difference $m_{\chi^+} - m_\chi$ is larger than 10 GeV/c^2;
- 69 GeV/c^2 for the second lightest neutralino, when it is higgsino-like and the mass difference $m_{\chi'} - m_\chi$ is larger than 10 GeV/c^2.

These results substantially extend the domains previously excluded at LEP1 [7, 8, 20, 21].

Acknowledgements

We wish to thank and congratulate our colleagues from the accelerator divisions for having been so fast and efficient in bringing up and operating LEP in this new energy regime. We are indebted to the engineers and technicians in all our institutions for their contribution to the excellent performance of ALEPH. Those of us from non-member countries thank CERN for its hospitality.

References

[1] For a compilation of review articles, see: *Supersymmetry and Supergravity*, Ed. M. Jacob, North-Holland and World Scientific, 1986.

[2] J. Ellis, K. Enqvist, D. Nanopoulos and F. Zwirner, *Mod. Phys. Lett.* **A 1** (1986) 57;
R. Barbieri and G.F. Giudice, *Nucl. Phys.* **B 306** (1988) 63;
S. Dimopoulos and G.F. Giudice, *Phys. Lett.* **B 357** (1995) 573.

[3] G. Farrar and P. Fayet, *Phys. Lett.* **B 76** (1978) 575.

[4] J. Ellis and S. Rudaz, *Phys. Lett.* **B 128** (1983) 248.

[5] D0 Coll., *Search for Squarks and Gluinos in $p\overline{p}$ collisions at the D0 Detector*, contributed paper No. 434 to the Int. Europhysics Conf. on High Energy Physics, Brussels (Belgium), July 27 - August 2, 1995;
CDF Coll., *Exotic Physics at CDF*, contributed paper No. 769, *ibid.*

[6] See for instance: H.P. Nilles, *Phys. Rep.* **110** (1984) 1;
H.E. Haber and G.L. Kane, *Phys. Rep.* **117** (1985) 75;
R. Barbieri, *Riv. Nuovo Cim.* **11** no.4 (1988) 1.

[7] ALEPH Coll., D. Decamp *et al.*, *Phys. Rep.* **216** (1992) 253.

[8] ALEPH Coll., *Search for scalar top quarks in e^+e^- collisions at LEP1 energies*, contributed paper No. 416 to the Int. Europhysics Conf. on High Energy Physics, Brussels (Belgium), July 27 - August 2, 1995.

[9] S. Katsanevas and S. Melachroinos, `SUSYGEN`, to appear in the Proceedings of the Workshop *Physics at LEP2*, CERN, 1995,
Eds. G. Altarelli, T. Sjöstrand, and F. Zwirner.

[10] E. Barberio and Z. Was, *Comp. Phys. Comm.* **79** (1994) 291.

[11] T. Sjöstrand, *Comp. Phys. Comm.* **82** (1994) 74.

[12] R. Miquel and M. Schmitt, *Four fermion production through resonating boson pairs at LEP2*, CERN-PPE/95-109, to be published in *Z. Phys.* **C**.

[13] ALEPH Coll., D. Buskulic *et al.*, *Phys. Lett.* **B 313** (1993) 509.

[14] J.M. Hilgart, R. Kleiss and F. Le Diberder, *Comp. Phys. Comm.* **75** (1993) 191.

[15] ALEPH Coll., D. Decamp *et al.*, *Nucl. Instr. Meth.* **A 294** (1990) 121.

[16] ALEPH Coll., D. Buskulic *et al.*, *Nucl. Instr. Meth.* **A 360** (1995) 481.

[17] VENUS Coll., N. Hosada *et al.*, *Phys. Lett.* **B 331** (1994) 211,
and earlier references therein.

[18] A. Bartl, H. Fraas and W. Majerotto, *Z. Phys.* **C 30** (1986) 441;
Nucl. Phys. **B 278** (1986) 1.

[19] W.A. Bardeen, M. Carena, S. Pokorski and C.E.M. Wagner,
Phys. Lett. **B 320** (1994) 110.

[20] L3 Coll., M. Acciarri *et al.*, *Phys. Lett.* **B 350** (1995) 109.

[21] OPAL Coll., R. Akers *et al.*, *Phys. Lett.* **B 337** (1994) 394.

m_χ in GeV/c^2	0	30	55
Selectrons	72	71	40
Smuons	74	75	45
Staus	59	54	7

Table 1: Selection efficiencies, in percent, for 60 GeV/c^2 mass sleptons and for three neutralino masses, at a centre-of-mass energy of 133 GeV.

m_χ in GeV/c^2	0	30	60
$H-H$	44	75	21
$H-\ell$	74	80	21
$H-\tau$	62	70	6
$\ell-\ell$	75	71	6
$\ell-\tau$	61	52	3
$\tau-\tau$	53	40	1
W*	58	74	17

Table 2: Selection efficiencies, in percent, for 65 GeV/c^2 mass charginos and for three neutralino masses, at a centre-of-mass energy of 133 GeV. The decay channels are labelled H for hadrons, ℓ for electrons and muons, τ for taus. The label W* corresponds to a weighting of the various channels assuming W-exchange dominance in the chargino decays.

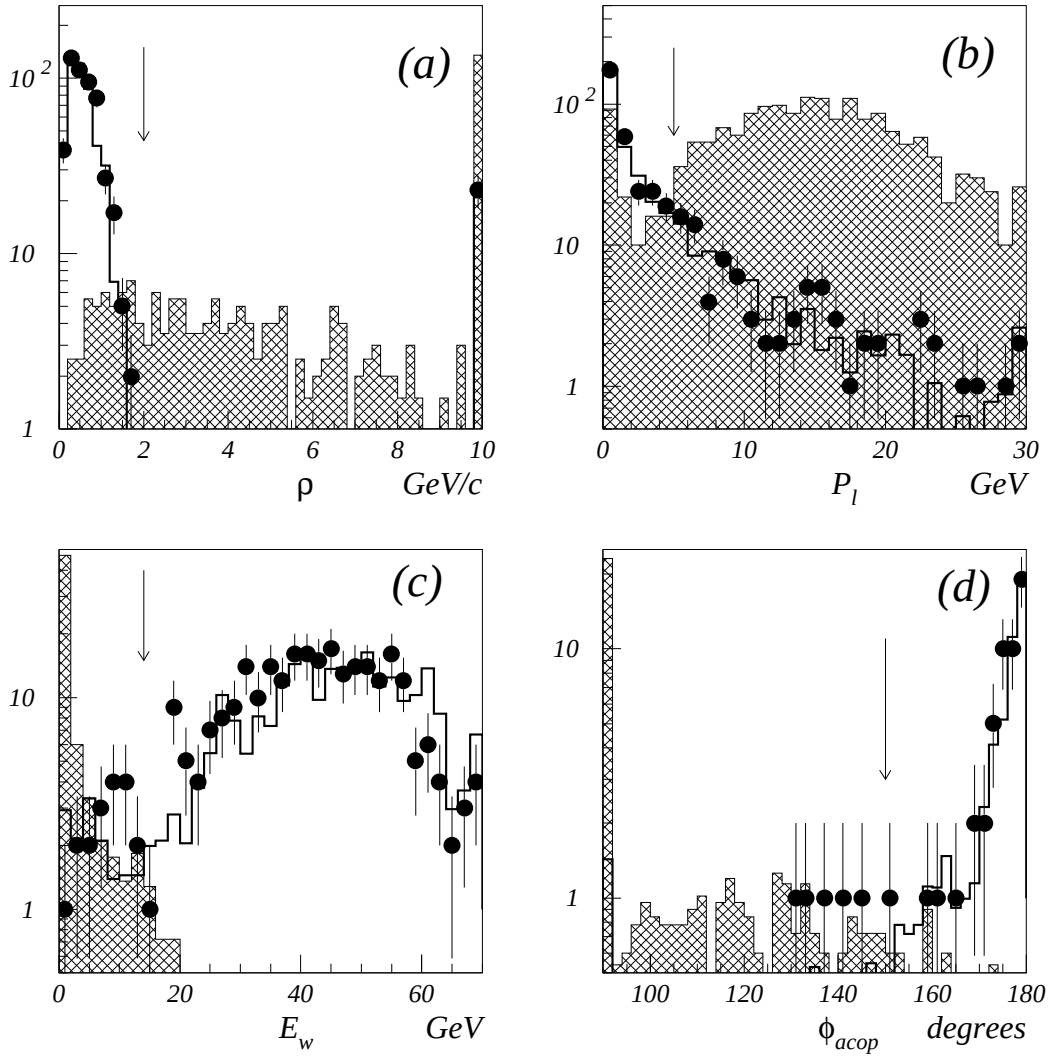

Figure 1: Discriminating variables used in the topological searches. The points with error bars represent the data, the histograms the background Monte Carlo expectations, with an absolute normalization, and the hatched histograms the signal expectations, with an arbitrary normalization. The arrows indicate the cut locations. Top left (a): the ρ variable used in the acoplanar lepton pair search; top right (b): the lepton momentum used in the search for isolated leptons in hadronic events; bottom left (c): the E_w variable used in the search for hadronic events with missing energy; and bottom right (d): the projected acoplanarity angle used in the search for acoplanar jets. Overflows are contained in the rightmost bin in (a), (b) and (c), and underflows in the leftmost bin in (d). In these illustrative plots, only subsets of the cuts applied to the other variables were used, in order to preserve sufficient statistics. For the signal expectations, the masses of the smuon (a) and of the chargino (b and c) are 65 GeV/c^2, and the χ' mass (d) is 80 GeV/c^2; the χ mass is 30 GeV/c^2 in (a), (b) and (c), and 45 GeV/c^2 in (d); the centre-of-mass energy is 133 GeV.

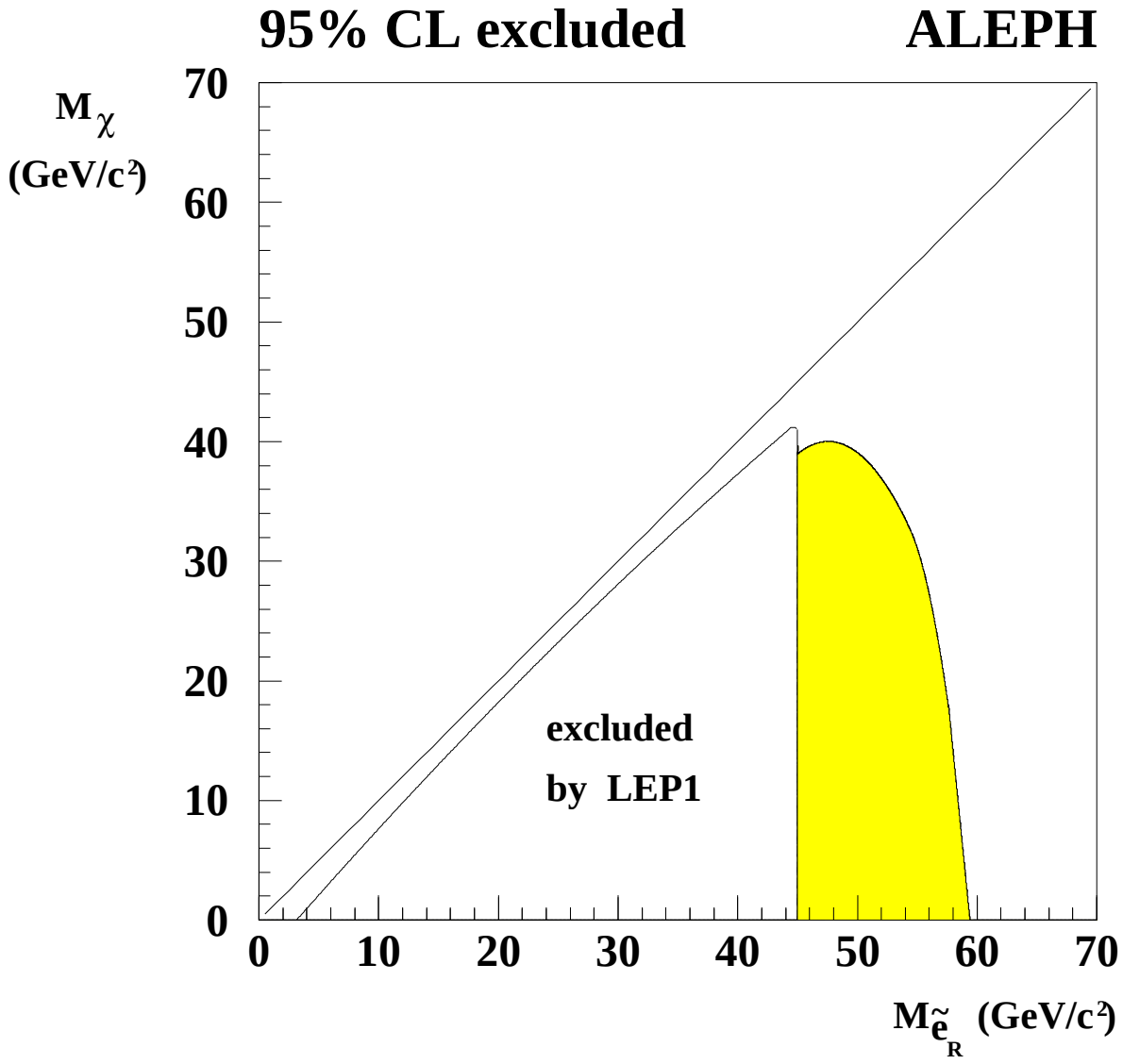

Figure 2: Domain excluded in the plane of the χ mass *vs.* the right selectron mass, in the deep gaugino region ($\mu = 1$ TeV/c^2, $\tan\beta = 2$). The limit from LEP1 is indicated, and the additional domain excluded by this analysis is shown shaded.

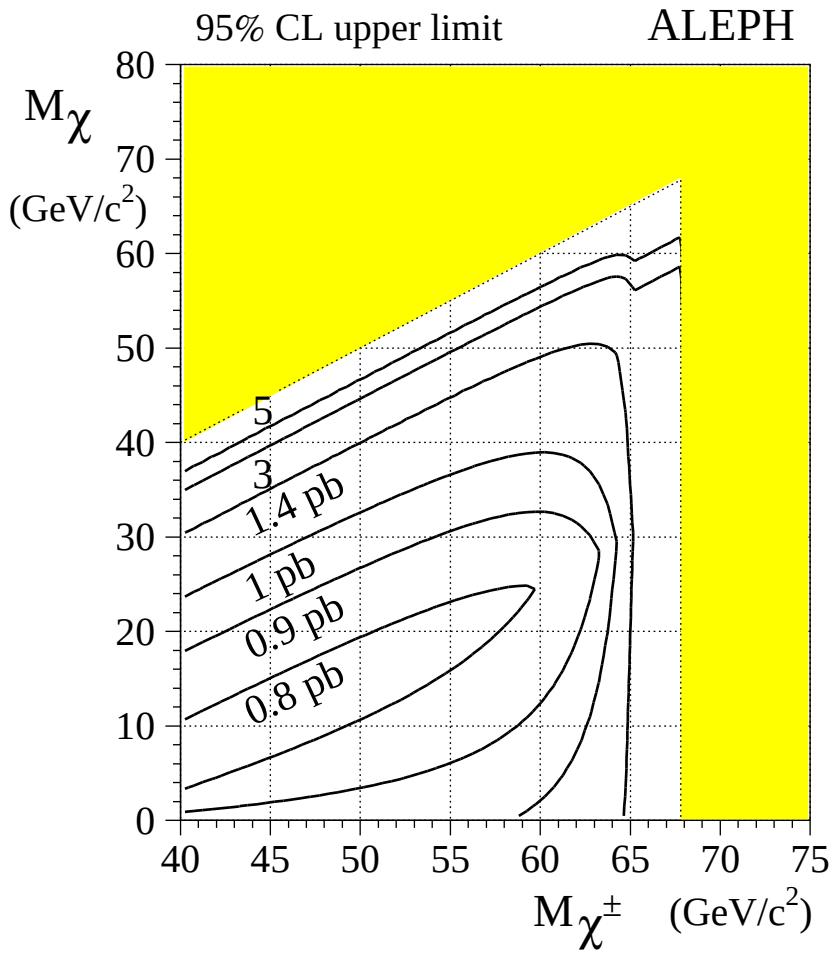

Figure 3: Limit on the chargino production cross section at $\sqrt{s} = 136$ GeV, assuming W* exchange dominance in chargino decays, as a function of the chargino and neutralino masses. The lines show the upper limit at the 95% confidence level. The shaded region is kinematically forbidden.

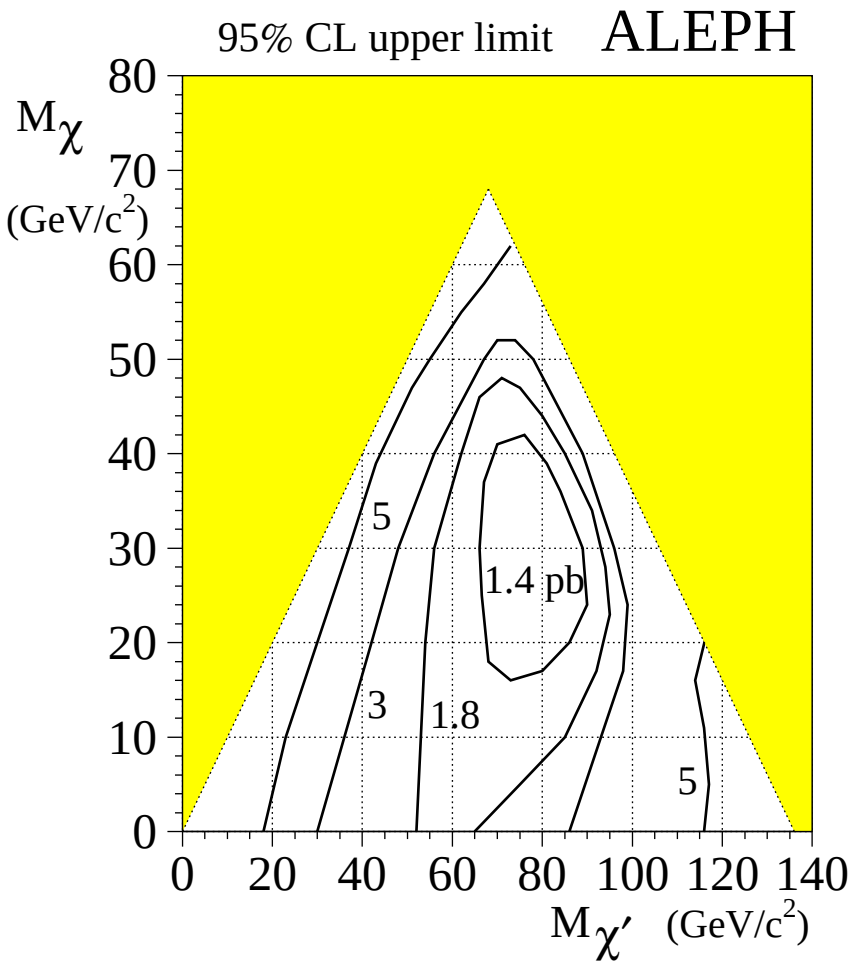

Figure 4: Limit on the associated neutralino production cross section at $\sqrt{s} = 136$ GeV, assuming Z^* exchange dominance in χ' decays, as a function of the neutralino masses. The lines show the upper limit at the 95% confidence level. The shaded region is kinematically forbidden.

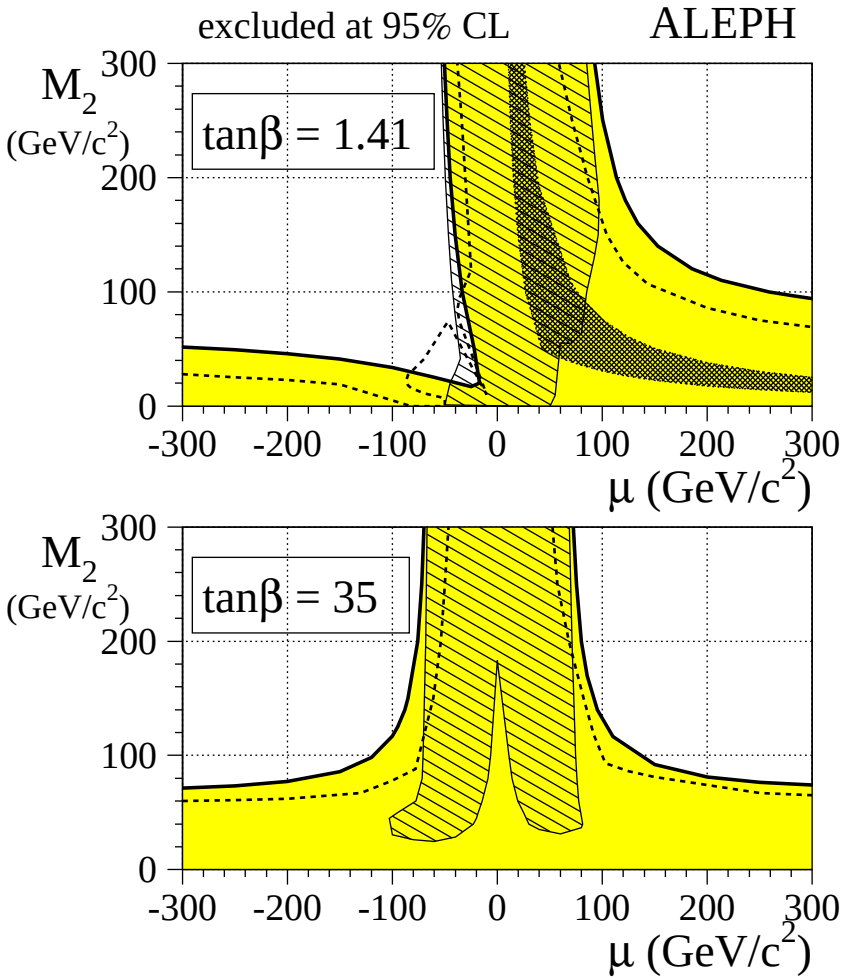

Figure 5: Domains in the MSSM (μ, M_2) plane excluded by the chargino search (shaded region) and the neutralino search (hatched region), for two values of $\tan\beta$. The dashed line indicates the previous limit, obtained at LEP1. The dark area, also excluded at LEP1, corresponds to the case of a chargino ligher than all neutralinos. The slepton masses are set to 500 GeV/c^2.

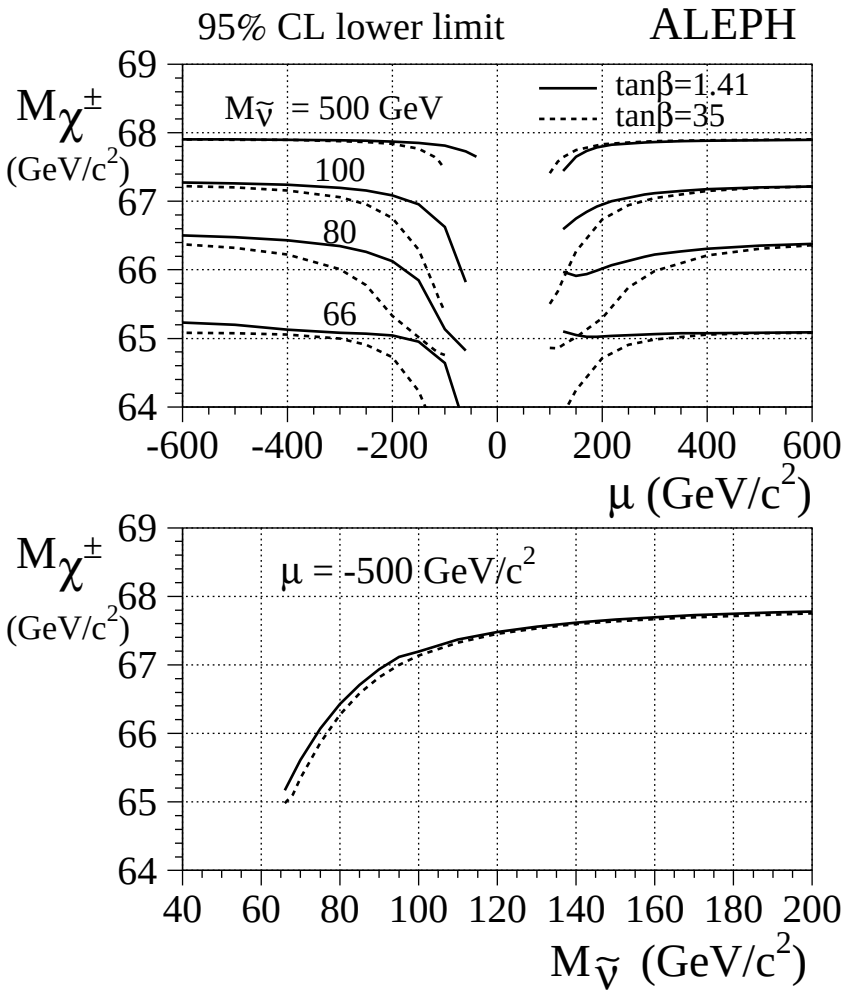

Figure 6: The lower limit on the chargino mass as a function of μ is shown in the upper plot. Four values of the sneutrino mass are considered, as indicated. The dependence on the sneutrino mass for a fixed value of μ is shown in the lower plot. The solid lines show the result for $\tan\beta = 1.41$, and the dashed lines for $\tan\beta = 35$.

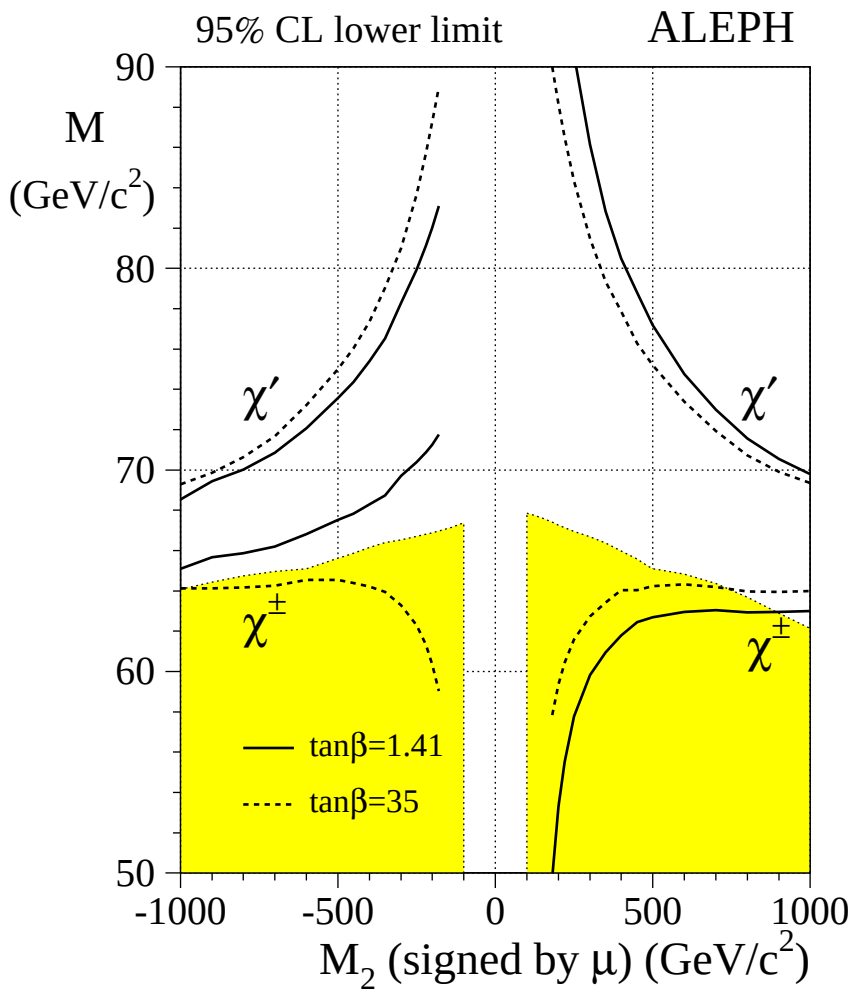

Figure 7: Lower limits on the chargino and neutralino masses as a function of M_2. The value of M_2 has been signed by μ, in order to show the limit for $\mu > 0$ and $\mu < 0$ together. The shaded region shows the chargino mass limit from the chargino search. The upper lines show the limit for the second neutralino. The lower lines show the limit on the chargino mass inferred from the neutralino search. The solid lines show the result for $\tan\beta = 1.41$, and the dashed lines, for $\tan\beta = 35$.